Available online at www.sciencedirect.com
ScienceDirect
Journal of Fluorine Chemistry 128 (2007) 459–464
JOURNAL OF FLUORINE CHEMISTRY
www.elsevier.com/locate/fluor

Review

Latest developments of bulk crystals and thin films of rare-earth doped CaF_2 for laser applications

J.L. Doualan [a], P. Camy [a], R. Moncorgé [a,*], E. Daran [b], M. Couchaud [c], B. Ferrand [c]

[a] *Centre Interdisciplinaire de Recherches sur les Ions et les Lasers (CIRIL), UMR 6637, CEA-CNRS-ENSICAEN, Université de Caen, 6 Blvd Maréchal Juin, 14050 Caen, France*
[b] *Laboratoire d'Analyse et d'Architecture des Systèmes (LAAS) du CNRS, 7 ave Colonel Roche, 31077 Toulouse, France*
[c] *LETI/DOPT/SCOPI/CDO, CEA-G, 17 rue des Martyrs, 38054 Grenoble Cedex 9, France*

Received 31 August 2006; received in revised form 12 December 2006; accepted 13 December 2006
Available online 14 January 2007

Abstract

Several CaF_2 single crystals doped with trivalent rare-earth ions have been grown in the recent years in the form of bulk crystals by using the Bridgman method and in the form of thin films by using the MBE and LPE techniques. The spectroscopic, gain and laser properties of these crystals doped with Pr^{3+}, on the one hand, and with Yb^{3+}, Tm^{3+} or Er^{3+} ions, on the other hand, have been studied and are reviewed here for their laser potentials in the red and in the infrared spectral domains, respectively.

Keywords: CaF_2; Crystal; Rare-earth ions; Luminescence; Laser

Contents

1. Introduction

CaF_2 (fluorine) is a well-known material and has been used for a long time in many optical components for its exceptional transparency in the UV as well as in the infrared spectral domain (see in Table 1). There is now, however, an increasing interest in the fabrication of ultrapure and large size single crystals for submicro-photolithography as well as in the fabrication of rare-earth doped bulk crystals and thin films for laser applications.

The reason for this renewing interest comes from the relative ease of growing this material in the form of bulk crystals and of thin films by using standard techniques such as the Bridgman and Czochralski techniques, on one hand, and the molecular beam epitaxy (MBE) [1] and liquid phase epitaxy (LPE) [2] techniques on the other hand.

Several other properties are also interesting when this material is doped with trivalent rare-earth ions. Because of a relatively low maximum phonon frequency (≈495 cm^{-1}), non-radiative relaxations between adjacent energy levels are very much reduced, thus allowing many visible and infrared optical transitions with large fluorescence quantum efficiencies. Moreover, when trivalent rare-earth ions are incorporated in CaF_2, charge compensation is required to maintain the electrical neutrality of the system. This leads to a complex

* Corresponding author. Tel.: +33 2 31 45 25 58; fax: +33 2 31 45 25 57.
E-mail address: richard.moncorge@ensicaen.fr (R. Moncorgé).

0022-1139/$ – see front matter © 2007 Elsevier B.V. All rights reserved.
doi:10.1016/j.jfluchem.2006.12.017

Table 1
Physical parameters of CaF_2

Structure	Cubic *Fm*-3*m* [5]
Cell parameter (nm)	0.5463
Molar mass (g)	78.08
Melting temperature (°C)	1360–1423 °C[a] [5,6]
Density (g/cm^3)	3.181
Transparency range	0.15–9 μm [5]
Refractive index	1.42 (1 μm) [5]
d*n*/d*t* (10^{-6} K^{-1})	−11.5 [7]
Therm. shock, R_T (W/m)	170
Hardness	4 Mohs or 158 Knopp [5,6]
Young module (GPa)	110 [7]
Therm. cond., κ (Wm^{-1} K^{-1})	9.7 [7]
Exp. coef., α (10^{-6} K^{-1})	26 or 16.2–19.4 [5,7]

[a]The experimental data for the melting temperature range between 1360 °C (most data) and 1423 °C (Handbook of Chemistry and Physics, 87th ed., CRC Press, 2006); some other temperatures are also often referred in between, such as 1402 and 1418 °C.

site structure, including so-called isolated ions (or monomers), pairs (or dimers) of adjacent rare-earth ions, trimers, tetramers, clusters, etc. depending on the nature of the rare-earth dopants and of the dopant concentration [3,4]. Such a complicated structure leads in turn to optical transitions having the form of broad-bands which can be used advantageously for the production of broadly tunable or short-pulse diode-pumped solid-state lasers.

As a matter of fact, CaF_2 appears as a very attractive laser host, which combines several advantages of fluoride crystals and glasses.

As mentioned above, since it can be grown rather easily either in the form of large dimension and good quality bulk crystals or in the form of thin films, and since it gives rise to rare-earth ion optical transitions having the form of broad bands, CaF_2 presents about the same advantages as glasses. At the same time, it keeps a number of advantages of single crystals (see in Table 1), among which (1) relatively large thermal conductivity and hardness, not as large as that found in the garnet crystals (the most commonly used solid-state laser hosts), for example, but significantly larger than that of glasses, and (2) rare-earth ion optical transitions with relatively large cross sections (see in the following). In addition, as in other fluoride systems such as $LiYF_4$ or $LiCaAlF_6$, it also presents a negative thermo-optic coefficient d*n*/d*T*, which means reduced thermal lensing effects at high power levels.

Among the variety of rare-earth dopant combinations which can be used to achieve laser action, we essentially addressed so far Yb^{3+}, for its broad band emission around 1 μm (used for ultra-short pulse laser applications), Tm^{3+} (in combination with Yb^{3+} or Y^{3+}), for its broad band emissions around 1.45 μm (telecom applications) and 1.9 μm (medical and LIDAR applications), and Er^{3+}, for its broad band emission around 2.8 μm (medical laser applications). More recently, however, we also studied Pr^{3+} doped crystals for their red laser emission around 605 nm (medical imaging and quantum computing applications). This is the reason why, various samples in the form of bulk crystals and/or of thin films were recently prepared and studied.

2. Material synthesis

Bulk crystals of about 1.5 cm diameter over 2–3 cm long are currently grown in our laboratory by using a standard Bridgman technique with RF heating and CF_4 + argon atmosphere (see in Fig. 1 for a typical crystal). Starting powders are commercially available CaF_2 and RE_2O_3 (with RE = Y, Er, Tm or Yb) powders with 4N purity [8].

Crystalline thin films were obtained by using both MBE and LPE techniques. In both cases, the films were deposited on commerciallly available CaF_2 substrates (from Kristalle Sensorik Optik Berlin, for example) with [1 1 1] orientation.

CaF_2 thin films with 13 wt% Er were initially deposited by using the MBE technique (LAAS laboratory) in order to study their gain and loss properties at $\lambda = 2.8$ μm [9]. These Er doped thin films were then protected by depositing an additional CaF_2 "cladding" with about the same thickness. Er doped thin films were 2.1 μm thick and 4 mm long. Er doping led to a refractive index about 2% larger than that of the pure CaF_2 substrate and cladding, allowing suitable wave-guiding properties without any other process.

LPE thin films were obtained by using a $CaCl_2$ solvant to lower the growth temperature (for an equimolar mixing of CaF_2 and $CaCl_2$) down to about 850 °C [10]. The growing system is made of two heating zones (resistive heating) with no temperature gradient between them. The Pt crucible is placed here within a quartz tube. Once the compacted powders are melted (around 870–885 °C), the solution is homogenized with the aid of a small Pt paddle, then the substrate is dipped inside the solution and maintained therein depending on the desired thin film thickness [11]. Rare-earth doping was realized by adding the desired quantity of rare-earth fluoride powder directly into the solution.

3. Infrared luminescence and laser properties of Yb^{3+}, Tm^{3+} and Er^{3+} doped CaF_2 crystals

Yb^{3+} luminescence essentially occurs in the near infrared. It is assigned to optical transitions (absorption and emission) between the crystal-field splitted components of the spin–orbit states $^2F_{5/2}$ and $^2F_{7/2}$. At the moment, Yb^{3+} luminescence has been only studied in bulk crystals [12]. When properly prepared, absorption spectra of bulk crystals only reveal the

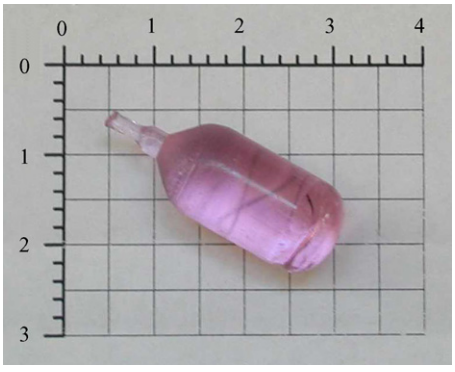

Fig. 1. Picture of a 1 cm diameter and 2 cm long Nd^{3+}:CaF_2 single crystal.

existence of Yb^{3+} ions. No trace of UV absorbing Yb^{2+} species can be detected.

As shown in Fig. 2, Yb^{3+} absorption is broad and relatively intense with a peak cross section of about 0.6×10^{-20} cm^2 around 980 nm. Such a cross section, for example, compares well with that found for Yb:YAG, a laser system which already led to a record continuous wave laser power of the order of 1 kW for which it is found 0.94×10^{-20} cm^2.

Moreover, as shown in Fig. 3, Yb^{3+} emission extends from about 900 to 1060 nm, with an emission cross section of about 0.7×10^{-20} cm^2 around 980 nm and 0.35×10^{-20} cm^2 around 1030 nm, and the fluorescence lifetime measured in a 5% Yb doped sample is of the order 2.4 ms. Such a broad band and such an emission cross section (2.0×10^{-20} cm^2 in the case of Yb:YAG) combined with such a long fluorescence lifetime (0.78 ms in the case of Yb:YAG) were recently found to be highly favourable not only for wide laser wavelength tunability [12] but also for ultra-short pulse and high average power laser operations [13,14]. A subsequent spectroscopic study [15] also proved that these exceptional laser properties, in spite of many possible incorporation sites, were essentially due, in these highly doped crystals (5% Yb^{3+}, typically), to only one luminescent species, the nature of which is not yet completely elucidated. According to this study, the considered luminescent center would be an hexameric type aggregate center [16] made of several Yb^{3+} neighboring ions.

Laser operation of Yb^{3+} was also achieved with crystals codoped with Nd^{3+} and Yb^{3+} ions [17]. The objective was to lase the Yb^{3+} ions at the shortest emission wavelengths after pumping the Nd^{3+} ions around 800 nm and $Nd^{3+} \rightarrow Yb^{3+}$ energy transfers. Efficient energy transfers, due to particular Nd^{3+}–Yb^{3+} clusters, were indeed proved and CW laser operation between 1030 and 1055 nm was obtained. The drawback of that system, however, was the non-negligible and detrimental fractions of Nd^{3+}–Nd^{3+} and Yb^{3+}–Yb^{3+} ion-pairs.

The situation is even more complicated in the case of Tm^{3+} doped CaF_2 for which samples have been grown, in the form of bulk crystals [18] and LPE thin films [19]. As shown in Fig. 3,

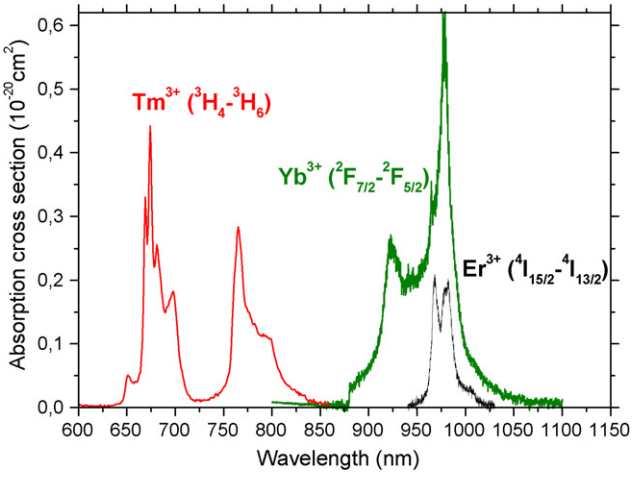

Fig. 2. Room temperature absorption spectra of Yb^{3+}, Tm^{3+} and Er^{3+} ions in CaF_2 around 800 and 980 nm (typical emission wavelengths of high power laser diodes).

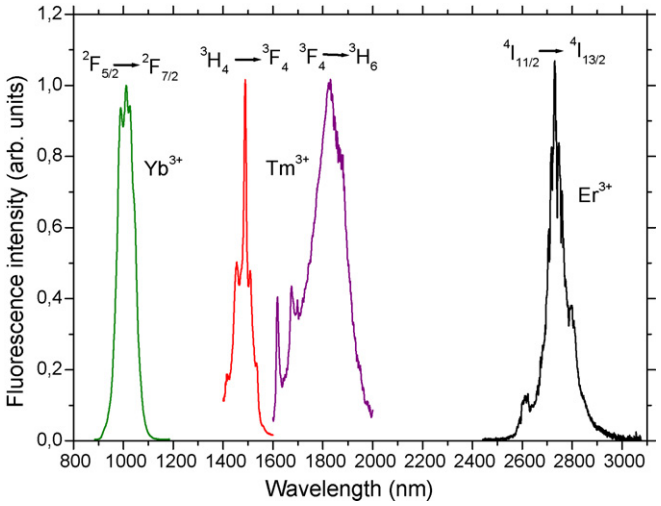

Fig. 3. Room temperature infrared emission spectra of Yb^{3+}, Tm^{3+} and Er^{3+} doped CaF_2.

two emissions may occur in the near infrared after $^3H_4$ excitation around 800 nm (see also in Figs. 4 and 5): (i) an emission extending from about 1.4 to 1.55 μm and peaking around 1.485 μm, which is assigned to a $^3H_4 \rightarrow {}^3F_4$ optical transition, and (ii) an emission extending from about 1.6 to 2 μm, peaking around 1.83 μm and assigned to a $^3F_4 \rightarrow {}^3H_6$ transition.

It is known, however, that these two emissions cannot be optimized together for the same dopant concentration. Indeed, due to efficient $^3H_4(1)$, $^3H_6(2) \rightarrow {}^3F_4(1)$, $^3F_4(2)$ cross-relaxation energy transfers [20] between adjacent Tm^{3+} ions above some concentration level (a few percents in general), the efficiency of the 1.9 μm emission is rapidly increasing at the expense of the 1.5 μm one. This is illustrated in Fig. 5 in which we have reported the Tm^{3+} emission spectra recorded in crystals with different dopant and codopant concentrations.

Quenching of the 1.5 μm emission due to cross-relaxation energy transfers is suitable when a 1.9 μm laser operation is desired (see in the following section). On the contrary, a low dopant concentration thus reduced cross-relaxation energy transfers are required for an efficient 1.5 μm emission. In this case, lasing operation can be achieved, however, by codoping the crystals with some other ions, such as Yb^{3+}, to reduce the

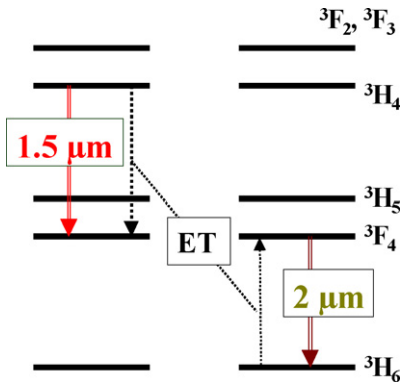

Fig. 4. Cross-relaxation energy transfer (ET) process and 1.5 and 2 μm laser transitions characteristic of Tm^{3+} doped materials.

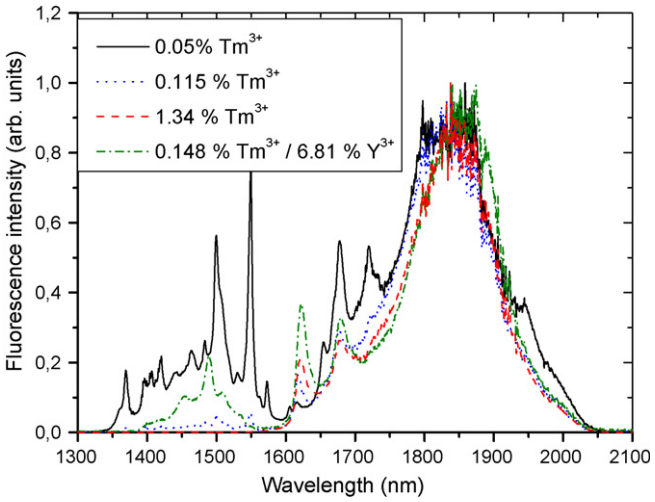

Fig. 5. Room temperature emission spectra of CaF_2 single crystals with various Tm^{3+} dopant concentrations and Y^{3+} codopants.

fluorescence lifetime of the $^3F_4$ terminal level of the laser transition, the one, otherwise, becomes much longer than that of the $^3H_4$ emitting level and results in some detrimental bottlenecking effect [20].

This question is even more critical in a system like CaF_2, since trivalent rare-earth dopants in this material tend to form pairs (even aggregates) of adjacent ions, for charge compensation, even at low dopant concentrations (see curves of Fig. 5 for 0.115 and 1.34% Tm^{3+}). In this case, codoping with non-optically active Y^{3+} ions (see curve of Fig. 5 for 0.148% Tm^{3+}, 6.81% Y^{3+}) was realized to reduce the number of Tm^{3+}–Tm^{3+} pairs in the crystal and to recover some $^3H_4$ emission around 1.5 μm. According to studies made in the past [3] concerning rare-earth ion pairs in CaF_2, it is believed that the Y^{3+} ions enter the lattice predominantly in the vicinity of the Tm^{3+} ions, as shown in Fig. 6.

Emission of Er:CaF_2 in the mid-infrared extends from 2.5 to 3 μm with a maximum around 2.73 μm. As we already reported in the past, this laser system can be pumped at various wavelengths, including around 1.5 μm, thus in the terminal level of the 2.8 μm laser transition (transition $^4I_{11/2} \rightarrow {}^4I_{13/2}$), due to complex cross-relaxation and upconversion energy transfers (see in Fig. 7). However, the best laser performance

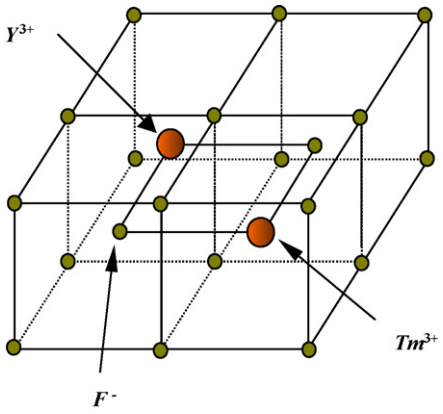

Fig. 6. Ion-pair in codoped Y, Tm:CaF_2.

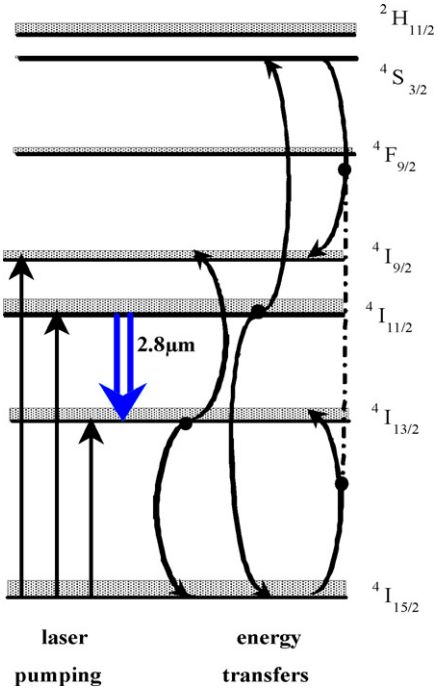

Fig. 7. Cross-relaxation and up-conversion energy transfer processes in Er:CaF_2.

were obtained by pumping the crystals around 980 nm (see in Fig. 2), thus directly into the $^4I_{11/2}$ laser level [21].

Concerning thin films, gain measurements were only performed so far in Er^{3+} doped MBE and in Tm^{3+} doped LPE thin films.

In the case of Er^{3+}, we only show here, as an illustration, the gain curve obtained at the laser wavelength $\lambda = 2.8$ μm in the Er^{3+}:CaF_2 MBE thin film described in Section 2 for a pumping wavelength of 970 nm (pump beam provided by a CW Ti:Sa laser). This crystalline planar waveguide was monomode for 2.8 μm and bimodal for 970 nm. The 2.8 μm probe beam was that of an home-made diode-pumped Er:CaF_2 laser based on a 3.9 mm thick 10.34% Er doped crystal [21] and a Cassegrain

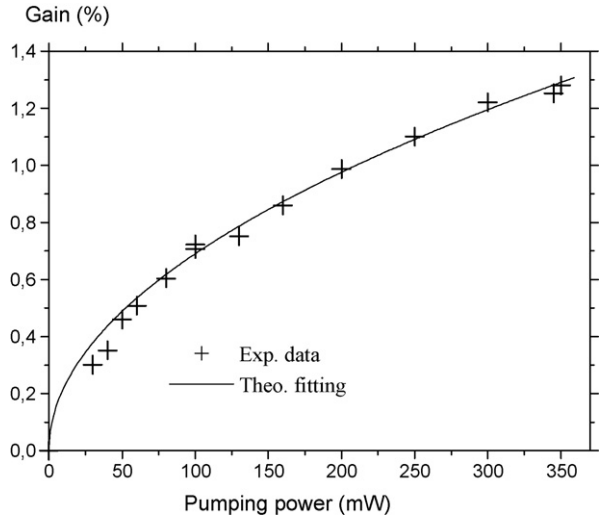

Fig. 8. Laser gain obtained at 2.8 μm in a Er:CaF_2 planar waveguide.

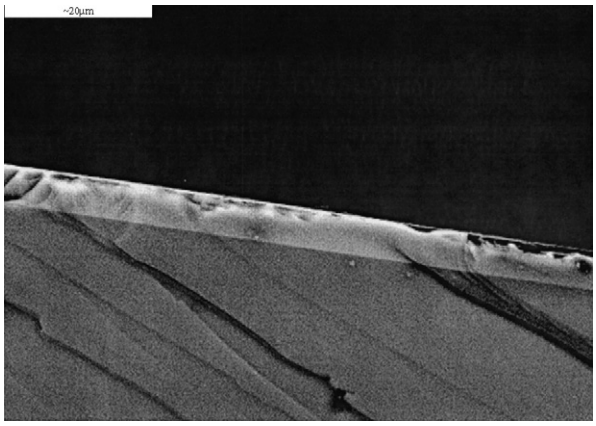

Fig. 9. SEM image of Tm^{3+}:CaF_2 thin-film over a CaF_2 substrate.

reflector was used to inject this probe light into the guide. As shown in Fig. 8, a saturation effect is observed resulting from the energy transfer induced non-linear variation of the $^4I_{11/2}$ excited level.

Concerning Tm^{3+}, gain measurements were performed around 1.9 μm by using a 5 mm long and 5 μm thick Er^{3+}, Tm^{3+} codoped planar waveguide with polished end-faces [19]. Fig. 9 shows a scanning electron microscope (SEM) image of such a thin-film deposited on a pure CaF_2 substrate. Fig. 10 shows the guiding trace obtained by injecting the pump light from a Ti-sapphire laser beam tuned at 765 nm, the observed fluorescence coming from the upconversion green emission of the Er^{3+} impurities. Injecting the probe light at 1.9 μm from an home-made Tm:YLF laser, 7% single-pass gain was obtained for 420 mW pump power.

4. Red luminescence and laser potential of Pr^{3+} doped CaF_2 crystals

Red luminescence in Pr^{3+} doped materials is usually assigned to the two metastable levels $^3P_0$ and $^1D_2$. We more particularly focused our attention, however, to the emissions

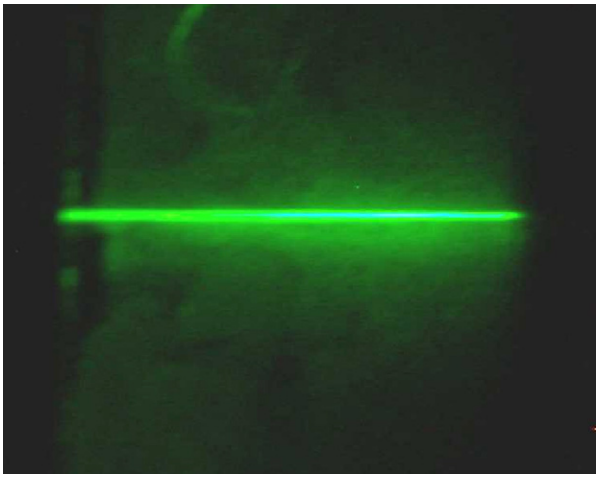

Fig. 10. Guiding trace in a Tm^{3+}, Er^{3+}:CaF_2 thin-film due to the parasitic upconversion green fluorescence of Er^{3+} impurities.

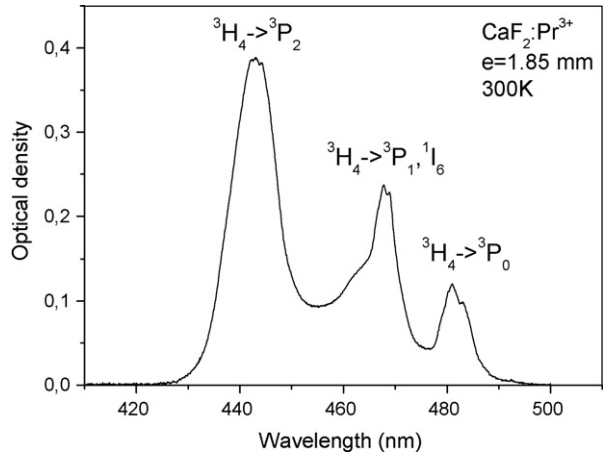

Fig. 11. Absorption bands of Pr^{3+}:CaF_2 around 450 nm.

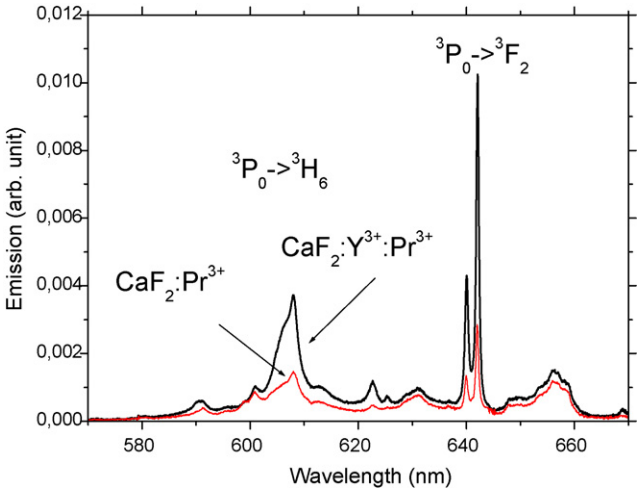

Fig. 12. Emission spectra of Pr^{3+} and (Y^{3+}, Pr^{3+}) doped crystals around 600 nm.

coming from level $^3P_0$ around 605 ($^3P_0 \rightarrow {}^3H_6$ optical transition) and 640 nm ($^3P_0 \rightarrow {}^3F_2$ transition) because of the possibility to pump this emitting level around 445 nm ($^3H_4 \rightarrow {}^3P_2$ absorption transition, see in Fig. 11) with the recently developed and now commercially available GaN based blue laser diodes. Two types of crystals were grown and studied: Pr^{3+} and (Y^{3+}, Pr^{3+}) doped crystals [22]. Co-doped crystals were fabricated to examine the beneficial effect of the optically inactive Y^{3+} ions onto the efficiency of the $^3P_0$ luminescence of the Pr^{3+} ions.

Both types of crystals led in fact to similar absorption and emission spectra. However, the emission efficiency is higher in the co-doped crystal than in the singly doped one (see in Fig. 12). This also manifests in the emission lifetime of the $^3P_0$ emitting level, since it is found a fluorescence lifetime of about 200 μs in the co-doped system for a value of 50 μs in the singly doped ones. This simply means that co-doping with Y^{3+} ions reduces the fraction of Pr^{3+} ion pairs and aggregates and increases the $^3P_0$ emission quantum efficiency by reducing the non-radiative decay channels due to the energy transfers among the Pr^{3+} ions. Such a broad-band system could be very attractive for diode-pumped picosecond laser operation.

5. Conclusion

The crystal growth, spectroscopic, gain and laser properties of CaF_2 single crystals have been reviewed and discussed. This shows that such crystals, though some of them have been studied for a long time, still motivate some interest and that such an interest may be growing in the future for large size laser systems as well as for micro-photonics because of their exceptional optical properties and because of the possibility to get them rather easily in the form of large size bulk crystals as well as in the form of thin films.

Acknowledgements

Works described in this review have been performed within the framework of several PhD thesis (C. Labbé, S. Renard, V. Petit, S. Khiari) and several research programs (PICS CNRS, CMDO CNRS network, AUF) and thanks are expressed to all of them.

References

[1] L.A. Bausa, G. Lifante, E. Daran, P.L. Pernas, Appl. Phys. Lett. 68 (23) (1996) 3242–3244.
[2] P. Rogin, J. Hulliger, J. Cryst. Growth 172 (1997) 200–208.
[3] P.J. Bendall, C.R.A. Catlow, J. Corish, P.W.M. Jacobs, J. Sol. Stat. Chem. 51 (1984) 159–169.
[4] J.P. Laval, A. Abaouz, B. Frit, A. Le Ball, J. Sol. Stat. Chem. 85 (1990) 133–143.
[5] Société CRYSTAL Gmbh (http://www.crystal-gmbh.com/).
[6] Société CRYSTAN (http://www.crystran.co.uk/).
[7] B.W. Woods, S.A. Payne, J.E. Marion, R.S. Hughes, L.E. Davis, J. Opt. Soc. Am. B 8 (5) (1991) 970–977.
[8] A. Braud, S. Girard, J.L. Doualan, R. Moncorgé, IEEE QE 34 (1998) 2246–2255.
[9] P. Camy, J.L. Doualan, E. Daran, B. Viallet, R. Moncorgé, OPTIX Conf. (Marseilles, France, 2001).
[10] Cook Mc-Murdie, in Phase diagrams for ceramists, vol. VII, NIST, Am. Ceram. Soc. Ed., 1969.
[11] B. Ferrand, B. Chambaz, M. Couchaud, Opt. Mater. 11 (1999) 101–114.
[12] V. Petit, J.L. Doualan, P. Camy, V. Menard, R. Moncorgé, Appl. Phys. B 78 (2004) 681–684.
[13] A. Lucca, M. Jacquemet, F. Druon, F. Balembois, P. Georges, P. Camy, J.L. Doualan, R. Moncorgé, Opt. Lett. 29 (2004) 1879–1881.
[14] A. Lucca, G. Debourg, M. Jacquemet, F. Druon, F. Balembois, P. Georges, P. Camy, J.L. Doualan, R. Moncorgé, Opt. Lett. 29 (2004) 2767–2769.
[15] V. Petit, P. Camy, J.L. Doualan, R. Moncorgé, J. Lumin. 123 (2007) 5–7.
[16] S.A. Kazanski, A.I. Ryskin, et al. Phys. Rev. B 72 (2005), 014127-11.
[17] V. Petit, P. Camy, J.L. Doualan, R. Moncorgé, Appl. Phys. Lett. 88 (2006), 051111-3.
[18] P. Camy, J.L. Doualan, S. Renard, A. Braud, V. Ménard, R. Moncorgé, Opt. Comm. 236 (2004) 395–402.
[19] S. Renard, P. Camy, J.L. Doualan, R. Moncorgé, M. Couchaud, B. Ferrand, Opt. Mater. 28 (2006) 1289–1291.
[20] A. Braud, S. Girard, J.L. Doualan, M. Thuau, R. Moncorgé, Phys. Rev. B 61 (2000) 5280–5292.
[21] C. Labbé, J.L. Doualan, P. Camy, R. Moncorgé, M. Thuau, Opt. Commun. 209 (2002) 193–199.
[22] S. Khiari, M. Velazquez, R. Moncorgé, J.L. Doualan, P. Camy, A. Ferrier, M. Diaf, J. Alloys Compd., in press.